The scaling functions for the β-relaxation process of supercooled liquids and glasses

1990 J. Phys.: Condens. Matter 2 8485

(http://iopscience.iop.org/0953-8984/2/42/025)

J. Phys.: Condens. Matter **2** (1990) 8485–8498. Printed in the UK

The scaling functions for the β-relaxation process of supercooled liquids and glasses†

W Götze

Physik-Department, Technische Universität München, D-8046 Garching, Federal Republic of Germany and Max-Planck-Institut für Physik und Astrophysik, D-8000 München, Federal Republic of Germany

Received 17 April 1990, in final form 14 June 1990

Abstract. The scaling equations which determine the master functions for the β-relaxation process within the mode coupling theory of supercooled liquids are reformulated such that a direct numerical solution becomes possible. Tables are presented that allow an accurate derivation of the scaling function and susceptibilities by elementary manipulations. As an example of their application the β-peak scenario as predicted by the theory is demonstrated.

Within the mode coupling theory of structural glass transitions a certain regime of supercooled liquid dynamics, referred to as a β-relaxation regime, was identified. In this regime conventionally defined correlation functions or fluctuating force kernels, formed with two variables C and D, can be written as

$$\phi_{CD}(t) = f^c_{CD} + h_{CD}G(t). \tag{1a}$$

Here the so-called non-ergodicity parameter f^c_{CD} and the critical amplitude h_{CD} reflect the specific properties of the system's microscopic structure and also of the variables C and D; but f_{CD} and h_{CD} are independent of time t. The time dependence is described by $G(t)$, which is independent of C and D. Equation (1a) is obtained as an exact asymptotic result of the non linear equations of motion near the glass transition. It holds for all pairs of variables $X = C, D$ for which the overlap with some product of density fluctuations $\rho_{\boldsymbol{q}}$ does not vanish $\langle X\rho_{\boldsymbol{q}_1}\rho_{\boldsymbol{q}_2}\ldots\rho_{\boldsymbol{q}_l}\rangle \neq 0$ [1]. There are corrections to the specified asymptotic law, which depend on all microscopic details of the system. The corrections are different for different pairs of variables C, D. At present it is not possible to calculate the size of the corrections for realistic systems. The function $G(t)$ depends sensitively on the microscopic details via a correlation scale c_σ and a time scale t_σ:

$$G(t) = c_\sigma g(t/t_\sigma). \tag{1b}$$

The two scales vary as power-law functions of the separation σ from the glass transition singularity; but this will not be considered in this paper. The scaling function g is

† This paper is dedicated to Professor W Wild on the occasion of his 60th birthday.

0953-8984/90/428485+14$03.50

not universal; but it depends regularly on one single number λ only. This λ, called exponent parameter, as well as f^c_{CD} and h_{CD} depend smoothly on the parameters specifying the system. For the model of a one component system, λ, f^c, h and σ can be expressed by complicated but mathematically well understood formulae in terms of the structure factor. In this sense these parameters can be considered as known regular equilibrium quantities. The strong temperature variations of spectra near the glass transition are caused by the strong variations of the two scales; and the non-trivial spectral shapes are given by the scaling function g. The latter obeys the scaling equation

$$\epsilon + \lambda z \, \mathrm{LT}[g(t)^2](z) + [zg(z)]^2 = 0. \tag{2}$$

Here $\epsilon = 1$ specifies the liquid side of the liquid to glass transition and $\epsilon = -1$ holds for the glass side. The Laplace transform LT for complex frequency z is used with the convention

$$\mathrm{LT}[g(t)](z) = g(z) = \mathrm{i} \int_0^\infty \mathrm{d}t \, \exp(\mathrm{i}zt) g(t) \qquad \mathrm{Im}z > 0. \tag{3a}$$

For real frequencies ω, with $z = \omega + i0$, one obtains

$$g(\omega + \mathrm{i}0) = g'(\omega) + \mathrm{i}g''(\omega). \tag{3b}$$

The spectrum g'' and the reactive part g' can also be obtained as Fourier transforms

$$g''(\omega) = \int_0^\infty \cos(\omega t) g(t) \, \mathrm{d}t \qquad g'(\omega) = \int_0^\infty \sin(\omega t) g(t) \, \mathrm{d}t. \tag{3c}$$

The susceptibility $\chi(\omega) = \chi'(\omega + \mathrm{i}\chi''(\omega)$ is related to $g(\omega)$ trivially: $\omega g(\omega) = \chi(\omega)$. For a more detailed discussion of the theory, of the original references and of possible applications to experiments, the reader is referred to a recent review [2].

Measurable quantities for which the preceding formulae are suggested to be applicable are dielectric functions, coherent and incoherent neutron scattering laws, and elastic moduli. These examples deal with auto-correlations and the variables $C = D$ refer, respectively, to the dipole moment, the particle density and tagged particle density, and the stress. The factorization property (1*a*) implies that the time variation of $\phi_{CC} - f_{CC}$ is the same for all these quite different quantities, up to the prefactor h_{CC}. Also the scaling behaviour, formulated by (1*b*), is a rather specific prediction. A first successful test of (1*b*) was reported for coherent neutron scattering properties of the glass-forming compound $CaKNO_3$ [3]. Dielectric loss measurements of a certain polymer follow (1*b*) and obey the predicted variations of the scales c_σ, t_σ quite well [4]. The factorization property was verified by neutron scattering [5] and also by molecular dynamics work for a binary alloy model [6]. Recently published dynamical light scattering experiments confirm (1*b*) qualitatively [7]. So by now it is evident that there are some systems where the preceding formulae apply qualitatively. It is obvious in particular that the experimental techniques for testing the theory are available. For these reasons it seems timely to present the precise theoretical results for the master function $g(t)$ and for the corresponding spectra g'', χ''. It is the purpose of this paper to extend the previous theory of the scaling equation (2), to provide the quantitative details for g, and to illustrate the results for the representative value $\lambda = 0.7$.

To begin the discussion, let us recall the results that were derived originally [8]. The properly normalized scaling function exhibits the short-time asymptotic expansion $g = g_1 + O(t^{3a})$, where

$$g_1(t) = (1/t^a) - A_1 t^a \tag{4a}$$

$$A_1 = \tfrac{1}{2}\epsilon/[\Gamma(1-a)\Gamma(1+a) - \lambda]. \tag{4b}$$

So in leading order the scaling function exhibits the same critical decay $g \sim 1/t^a$ for the liquid and for the glass. For long times the scaling function of the glass approaches a constant:

$$g(t \to \infty) = 1/\sqrt{1-\lambda} \qquad \epsilon = -1. \tag{5}$$

For the liquid there occurs another power-law divergency

$$g(t) = g_b(t) + O(1/t^{3b})\epsilon = +1 \tag{6a}$$

$$g_b(t) = -Bt^b + (B_1/B)/t^b \qquad B > 0 \tag{6b}$$

$$B_1 = (1/2)/[\Gamma(1+b)\Gamma(1-b) - \lambda]. \tag{6c}$$

The numbers $0 < a < 1/2, 0 < b \leq 1$ are the critical exponents of the theory related to the exponent parameter via

$$\Gamma(1-a)^2/\Gamma(1-2a) = \lambda = \Gamma(1+b)^2/\Gamma(1+2b). \tag{7}$$

The crossover from the critical decay to the von Schweidler behaviour $g(t) \sim -Bt^b$ for the liquid, requires the existence of a zero, to be denoted by t^*:

$$g(t^*) = 0 \qquad \epsilon = 1. \tag{8}$$

Similarly, the crossover from the sublinear critical susceptibility variation $\chi''(\omega \gg 1) \propto \omega^a$ to the von Schweidler asymptote $\chi''(\omega \ll 1) \propto 1/\omega^b$ implies the existence of a susceptibility minimum. Let us use the notations

$$\begin{aligned} &\partial\chi''(\omega)/\partial\omega = 0 \quad \omega = \omega^* \\ &\chi^* = \chi''(\omega^*) \qquad \epsilon = +1. \end{aligned} \tag{9}$$

The four numbers B, t^*, ω^* and χ^* are examples of parameters specifying the liquid-state β dynamics. These numbers are given by λ, or, equivalently by one of the exponents a or b. Experimental test of the predicted connection of, say, a with one of the four numbers would be a rather direct check of the relevance of the theory. So far the mentioned connections were unknown and tests of the function $g(t)$ relied on verifying the leading power-law behaviour and the equation (7) relating the two fractal dimensionalities a and b. But it is much more advisable to test the theory in the intermediate range $t \sim t^*, \omega \sim \omega^*$ for the following reason. Results (1a) and (1b) hold only asymptotically in the scaling limit $\sigma \to 0, t/t_\sigma$ fixed [1]. In an experiment one gets $\sigma \neq 0$ results, which are spoiled by unknown corrections to the scaling laws. Such corrections occur for $t \to 0$, because of microscopic transient effects. They occur also for $t \to \infty$ because there the α relaxation process takes over. The corrections to

the asymptotic laws are smallest in the center of the β region, specified by ω^* or t^*. Previously the intermediate region was described by the ad hoc interpolation formula $g_{\rm int}(t) = (1/t^a) - Bt^b$, using B as a free fit parameter [9]. This simple expression is useful as a first attempt for data analysis, in particular if there are large experimental uncertainties anyway. The quality of dielectric loss data presumably requires a more adequate description of $g(t)$. The formula implies, for example, $t^*_{\rm int} = (1/B)^{1/(a+b)}$. For $\lambda = 0.7$ one gets from the proper coefficient B, to be calculated below, $t^*_{\rm int} = 1.49$. The correct result, to be calculated below, is $t^* = 0.85$. This discrepancy is outside the error bars of the results in [7].

To proceed, let us consider the convolution integral

$$f(t) = \int_0^t g(t-\tau)g(\tau)\,\mathrm{d}\tau. \tag{10a}$$

The mentioned short-time expansion of $g(t)$ implies for the behaviour of $f(t)$:

$$f(t) = [\lambda/(1-2a)]t^{1-2a} - 2A_1\Gamma(1-a)\Gamma(1+a)t + \mathrm{O}(t^{1+2a}). \tag{10b}$$

In particular $f(t=0) = 0$, and therefore Laplace back transform yields for (2):

$$-\epsilon + \lambda g(t)^2 = \frac{\mathrm{d}}{\mathrm{d}t} f(t). \tag{10c}$$

This result makes it plain that the scaling equation is an implicit non-linear integro-differential equation. For the derivation of the power-law behaviour (4*a*) or (6*b*) the leading cancellation of the two non-linear terms in (2) is essential. In order to restore the symmetric role of these two terms one can integrate (10*c*). In this manner one reformulates the scaling equation into the following equivalent form

$$\lambda \int_0^t g(\tau)^2\,\mathrm{d}\tau - \int_0^t g(t-\tau)g(\tau)\,\mathrm{d}\tau = \epsilon t \tag{11a}$$

$$\lim_{t\to 0} t^a g(t) = 1. \tag{11b}$$

The causality of the β-relaxation theory is now quite transparent: the properties of $g(t)$ for $t > t_0$ do not enter the equation for the master function on the time interval $0 < t \le t_0$. The crucial retardation effects are expressed by the convolution integral: all the properties of $g(\tau)$ for $0 < \tau < t$ are needed to determine $g(t)$. Formula (11*a*) is most convenient for extending the expansion (4*a*):

$$g(t) = g_n + \mathrm{O}(t^{(2n+1)a}) \tag{12a}$$

$$g_n(t) = (1/t^a) - A_1 t^a + A_2 t^{3a} - \cdots + (-1)^n A_n t^{(2n-1)a}. \tag{12b}$$

For the coefficients A_κ one obtains the recursion relation [7]:

$$A_\kappa = -\frac{1}{2}\sum_{\nu=1}^{\kappa-1} A_\nu A_{\kappa-\nu}\left[\Gamma(1+x_\kappa)\Gamma(1+x_{\kappa-\nu}) - \lambda\Gamma(1-a+x_\kappa)\right] \times \left[\Gamma(1-a)\Gamma(1+x_\kappa) - \lambda\Gamma(1-a+x_\kappa)\right]^{-1}. \tag{13}$$

Here $x_\kappa = -a + 2\kappa a$. Fourier transformation gives corresponding expansions for the susceptibility:

$$\chi''(\omega) = \chi''_n(\omega) + \mathrm{O}(1/\omega^{(2n+1)a}) \tag{14a}$$

$$\chi''_n(\omega) = A''_0\omega^a - A''_1/\omega^a + \cdots + (-1)^n A''_n/\omega^{(2n-1)a} \tag{14b}$$

$$A''_\kappa = -A_\kappa \sin(\pi x_\kappa/2)\Gamma(1 + x_\kappa). \tag{14c}$$

In the analogous formulae for $\chi'(\omega)$ enter the coefficients:

$$A'_\kappa = -A_\kappa \cos(\pi x_\kappa/2)\Gamma(1 + x_\kappa). \tag{14d}$$

For an efficient numerical treatment of the scaling equation it is preferable to avoid convolutions of two singular functions. This goal can be achieved by splitting $g(t)$ in some known singular part and a more regular remainder. In the following the version below will be applied:

$$g(t) = g_1(t) + g_r(t). \tag{15a}$$

From (11a) one reformulates the scaling equation as one for the function g_r:

$$2\int_0^t \{g_r(t-\tau) - \lambda g_r(\tau)\}\, g_1(\tau)\, \mathrm{d}\tau + \int_0^t \{[g_r(t-\tau) - \lambda g_r(\tau)]\, g_r(\tau)\}\, \mathrm{d}\tau + A_{11}t^{1+2a} = 0 \tag{15b}$$

$$A_{11} = A_1^2\left[(\Gamma(1+a)^2/\Gamma(1+2a)) - \lambda\right]/(1+2a). \tag{15c}$$

The remainder function exhibits the asymptotic behaviour $g_r(t) = A_2 t^{3a} + \mathrm{O}(t^{5a})$. A discretization of the preceding equation has been performed as follows. On a grid $t_j = h \cdot j$, $j = 0, 1, 2, \ldots$, the function g_r is approximated by a polygon, interpolating linearly between the values $g_r(t_j) = g_j$. Since then the curly brackets in (15b) reduce to piecewise linear functions one can carry out the integrals easily. As a result the scaling equation (15b) reduces to a quadratic equation for $y = g(t_n)$: $(-\lambda h/2)y^2 + C_n y + D_n = 0$. Here C_n is given in terms of A_1, λ and h. The coefficient D_n can be expressed in terms of A_{11}, h as well as all the g_j with $j < n$. Solving the elementary equation yields y in terms of $g_1, g_2, \ldots, g_{n-1}$. The procedure was started with g_1, evaluated from the approximation $g(h) \approx g_3(h)$. A step size $h = 0.1$ was sufficient to fix $g(t)$ with an accuracy of 10^{-4}. Since the algorithm is very efficient, it was not improved any further by the obvious possibility of increasing the stepsize with increasing t. The Fourier transforms (3c) are evaluated as follows. First one splits off the long-time asymptote by writing $g = f_c + \delta g$ for $\epsilon = -1$ and $g = g_b + \delta g$ for $\epsilon = +1$. Then a filter is introduced to isolate the short-time singularity: $\delta g(t) = F(t/\tau)\delta g(t) + \delta g_c(t)$. Here $F(t) = (1+t)\exp -t$ was chosen and τ was adjusted such that $F(t/\tau)\delta g(t) \approx F(t/\tau)\delta g_3(t)$. Here δg_3 is obtained from g_3 in (12a) by the proper subtractions. Then all integrals can be worked out analytically, except for the one involving $\delta g_c(t)$. The latter is done approximately, by replacing δg_c in (3c) by a polygon.

Some further mathematical comments concerning the scaling equation may be of interest. One can work out from (13) the asymptotic behaviour of the coefficients A_κ for large κ in order to understand that $g_n \to g(t)$ on a finite non-zero interval $0 < t < t_1$. So there is a solution of (11) on a non-trivial time interval, and it can be

Table 1. Relationship between the exponent parameter λ and the exponents a and b (equation (7)). See the text for details.

λ	a	b	λ	a	b
0.500	0.395	1.000	0.740	0.309	0.575
0.520	0.390	0.961	0.760	0.300	0.542
0.540	0.384	0.922	0.780	0.290	0.509
0.560	0.377	0.885	0.800	0.279	0.476
0.580	0.371	0.848	0.820	0.267	0.443
0.600	0.364	0.812	0.840	0.255	0.409
0.620	0.358	0.777	0.860	0.241	0.375
0.640	0.350	0.742	0.880	0.226	0.339
0.660	0.343	0.708	0.900	0.209	0.303
0.680	0.335	0.674	0.910	0.200	0.284
0.700	0.327	0.641	0.920	0.190	0.264
0.720	0.318	0.608	0.930	0.180	0.244

evaluated there with any desired accuracy from (12). Let us assume that there is a continuous function $g_0(t)$, defined for $0 < t \leq t_0$, which obeys (11) for $t \leq t_0$. Let us write $g_0(t) = F(t)/t^a$, so that $F(t)$ is continuous for $0 \leq t \leq t_0$ with

$$F(t) = 1 - A_1 t^{2a} + O(t^{4a}). \tag{16a}$$

Let us also write $t = t_0 + s$ and denote the continuation of g_0 by f:

$$g(t_0 + s) = f(s) \qquad 0 \leq s \leq t_0. \tag{16b}$$

Then (11) leads to the equation for f:

$$\int_0^s (s-\xi)^{-a} F(s-\xi) f(\xi)\, d\xi = i(s). \tag{16c}$$

Here the inhomogeneity consists of a known part i_0 and a simple non-linear term

$$i(s) = i_0(s) + \frac{1}{2}\lambda \int_0^s f(\xi)^2\, d\xi \tag{16d}$$

$$i_0(s) = \frac{1}{2}\left[\lambda \int_0^{t_0} g_0(\tau)^2\, d\tau - \int_s^{t_0} g_0(t_0 + \tau + s) g_0(\tau)\, d\tau - \epsilon(t_0 + s)\right]. \tag{16e}$$

This is a smooth function of s and $i(s = 0) = 0$. For given $i(s)$, equation (16c) is an example of a generalized Abel's equation. The standard theory of this equation yields the result for the unique solution in the form

$$f(s) = \int_0^s K(s-\tau)\left[i_0'(\tau) + (\lambda/2) f(\tau)^2\right] d\tau \tag{17}$$

where the kernel K can be expressed as some Neumann series. The proof, however, anticipates $F'(t)$ to be continuous, while the present F' exhibits a power-law divergency. I conjecture that this integrable singularity does not spoil the usual proof, so that (17) is an equivalent form for the scaling equation with a known weakly singular kernel K. Equation (17) has the same form as the Piccard integral equation except for the mentioned singularity. I further conjecture that this does not spoil the usual proof of existence and uniqueness of the solution of (17). By continuation, the method based on (16) can then be extended to any finite time interval. If one could prove the two conjectures one could put the theory of the β-process on a firm mathematical basis.

Table 2. The first three coefficients of the short-time expansion (12). See the text for details.

λ	ϵA_1	A_2	ϵA_3	λ	ϵA_1	A_2	ϵA_3
0.500	0.616	−0.053	0.0040	0.740	1.145	−0.150	0.0068
0.520	0.640	−0.057	0.0042	0.760	1.235	−0.170	0.0061
0.540	0.666	−0.061	0.0045	0.780	1.342	−0.194	0.0048
0.560	0.695	−0.065	0.0048	0.800	1.469	−0.225	0.0022
0.580	0.726	−0.070	0.0051	0.820	1.624	−0.264	−0.0027
0.600	0.761	−0.076	0.0054	0.840	1.816	−0.316	−0.0119
0.620	0.799	−0.083	0.0058	0.860	2.062	−0.387	−0.0292
0.640	0.841	−0.090	0.0061	0.880	2.388	−0.489	−0.0635
0.660	0.888	−0.098	0.0064	0.900	2.842	−0.643	−0.1367
0.680	0.940	−0.108	0.0067	0.910	3.143	−0.753	−0.2040
0.700	1.000	−0.120	0.0069	0.920	3.518	−0.898	−0.3112
0.720	1.067	−0.133	0.0069	0.930	3.997	−1.096	−0.4907

Table 3. Coefficients for the long-time asymptote (6*b*). See the text for details.

λ	B	B_1	t^*	λ	B	B_1	t^*
0.500	0.228	0.000	1.571	0.740	0.861	0.448	0.683
0.520	0.255	0.021	1.508	0.760	0.974	0.523	0.597
0.540	0.284	0.044	1.443	0.780	1.107	0.610	0.512
0.560	0.317	0.069	1.376	0.800	1.266	0.715	0.427
0.580	0.353	0.096	1.308	0.820	1.459	0.843	0.344
0.600	0.393	0.126	1.237	0.840	1.700	1.002	0.264
0.620	0.438	0.158	1.164	0.860	2.006	1.207	0.1898
0.640	0.488	0.194	1.088	0.880	2.410	1.480	0.1243
0.660	0.545	0.234	1.011	0.900	2.967	1.864	0.0704
0.680	0.609	0.278	0.932	0.910	3.333	2.120	0.0488
0.700	0.681	0.327	0.851	0.920	3.784	2.442	0.0313
0.720	0.765	0.384	0.767	0.930	4.355	2.857	0.0180

The result of the numerical work will be presented in the form of tables. These contain a complete list of that information necessary for the reader to construct all functions by himself by elementary manipulations with an error of the the order of 1%. Table 1 presents the relation (7) between exponent parameter λ and the exponents a and b. Table 2 presents the first three coefficients for the short-time expansion (12). Table 3 gives the two coefficients for the long-time asymptote (6*b*) of the liquid as well as the zero, (8), for the correlation function. B and t^* have been read off from the solution of (15). Since in all cases t^* is below the radius of convergence t_1 of the series (12*b*), one can calculate it also by pushing the series expansion to sufficiently high order. The numbers in table 2, if necessary after interpolation, allow the evaluation of g_3, (12*b*). This approximation works up to times close to the radius of convergence t_1. Not much can be gained on the usual logarithmic abscissa if one extends the expansion to g_n with $n > 3$. The numbers from table 3 allow the evaluation of the long-time asymptote g_b, (6*b*). In principle one can also extend the series (6) to higher order. But since this series is divergent, nothing is gained in this manner. It turns out that near t_1 both expansions g_3 and g_b match with an accuracy of about 1%. This is illustrated in figure 1. So the tables provide the master functions $g(t)$ easily with the specified accuracy, and series expansion cannot improve this result. Figure 2 shows the master

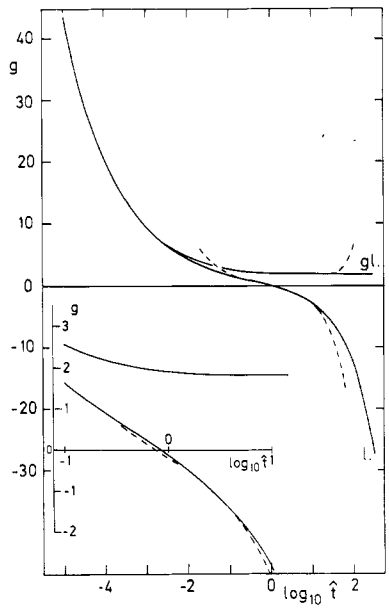

Figure 1. Scaling function g versus $\log_{10}\hat{t}$ for $\lambda = 0.7$. The broken curves are the asymptotic expressions g_3 and g_b respectively.

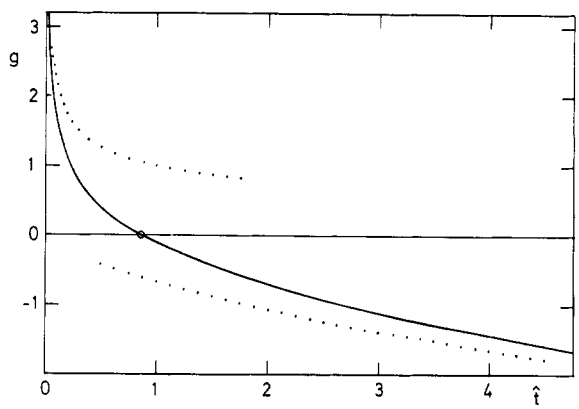

Figure 2. Scaling function g versus time $\hat{t}$ for $\lambda = 0.7$. The dotted curves represent respectively the critical decay $1/\hat{t}^a$ and the von Schweidler decay $-B\hat{t}^b$.

curve for $\lambda = 0.7$ on a linear abscissa. On such a presentation, which covers a bit more then one decade time variation, one cannot safely identify the leading asymptotes $1/t^a$ or $-Bt^b$. Both figures show that a save experimental test of the β-relaxation requires the detection of $g(t)$ over three to four decades. This is a severe problem reflecting the relaxation stretching. The latter is the very essence of glassy dynamics.

In table 4 all the coefficients needed to evaluate the susceptibility approximation χ_3, (14), are compiled. Fourier transformation of (6*b*) yields the low frequency result of the susceptibility, the von Schweidler behaviour and its first correction term: $\chi(\omega) =$

Table 4. Coefficients required to evaluate the susceptibility approximation (equation (14)). See the text for details.

λ	A_0''	$\epsilon A_1''$	A_2''	$\epsilon A_3''$	A_0'	$\epsilon A_1'$	A_2'	$\epsilon A_3'$
0.500	0.860	−0.318	0.056	−0.0003	−1.203	−0.444	−0.0167	0.0078
0.520	0.842	−0.326	0.059	−0.0007	−1.200	−0.465	−0.0161	0.0080
0.540	0.823	−0.335	0.063	−0.0011	−1.197	−0.488	−0.0153	0.0083
0.560	0.804	−0.345	0.068	−0.0015	−1.194	−0.512	−0.0143	0.0085
0.580	0.785	−0.356	0.073	−0.0020	−1.191	−0.539	−0.0131	0.0087
0.600	0.765	−0.367	0.078	−0.0026	−1.188	−0.569	−0.0116	0.0089
0.620	0.745	−0.379	0.085	−0.0031	−1.184	−0.602	−0.0097	0.0090
0.640	0.725	−0.392	0.092	−0.0037	−1.181	−0.639	−0.0074	0.0091
0.660	0.704	−0.406	0.100	−0.0043	−1.177	−0.680	−0.0045	0.0090
0.680	0.682	−0.422	0.109	−0.0049	−1.174	−0.726	−0.0009	0.0088
0.700	0.660	−0.439	0.119	−0.0055	−1.170	−0.778	0.0036	0.0085
0.720	0.637	−0.458	0.131	−0.0059	−1.165	−0.838	0.0092	0.0079
0.740	0.613	−0.479	0.145	−0.0061	−1.161	−0.907	0.0164	0.0070
0.760	0.589	−0.503	0.161	−0.0058	−1.156	−0.988	0.0257	0.0058
0.780	0.563	−0.530	0.181	−0.0047	−1.152	−1.084	0.0377	0.0040
0.800	0.537	−0.561	0.205	−0.0022	−1.146	−1.198	0.0537	0.0016
0.820	0.509	−0.598	0.234	0.0028	−1.141	−1.339	0.0754	−0.0016
0.840	0.480	−0.641	0.272	0.0124	−1.134	−1.514	0.1055	−0.0057
0.860	0.449	−0.693	0.321	0.0306	−1.128	−1.740	0.1489	−0.0102
0.880	0.416	−0.757	0.387	0.0661	−1.120	−2.041	0.2141	−0.0138
0.900	0.379	−0.841	0.481	0.1392	−1.112	−2.463	0.3183	−0.0103
0.910	0.360	−0.892	0.545	0.2040	−1.107	−2.744	0.3953	−0.0003
0.920	0.340	−0.954	0.625	0.3042	−1.102	−3.095	0.4994	0.0233
0.930	0.318	−1.028	0.729	0.4655	−1.097	−3.547	0.6453	0.0753

$\chi_b(\omega) + O(\omega^{3b})$. Here

$$\chi_b''(\omega) = (B_0''/\omega^b) + B_1''\omega^b \tag{18}$$

and a corresponding expression holds for χ_b'. The necessary coefficients are compiled in table 5 together with the parameters for the susceptibility minimum. For the glass the low frequency susceptibility can be determined by moment expansions.

$$g''(\omega) = c_0 - \tfrac{1}{2}c_2\omega^2 + O(\omega^4) \tag{19a}$$

$$g'(\omega) = (-f_c/\omega) + c_1\omega^1 + O(\omega^3) \qquad \epsilon = -1. \tag{19b}$$

The moments are listed in table 6. One can achieve matching of the various asymptotic formulae with an error in the region of 1–5% level. This is illustrated in figure 3. One notices again that the dynamics has to be studied over at least three decades in order to safely determine the relevant part of the β-spectrum.

Let us demonstrate the applicability of the presented results and complete the earlier discussion of the β-relaxation process by three figures. Figures 4 and 5 show as full curves the density correlator $\phi(t)$ and the tagged particle density correlator $\phi^s(t)$ evaluated numerically as solution of the full mode coupling equations for a certain schematic model (curves G in figure 3 of [9] and in figure 5 of [10]). Figure 6 shows a double logarithmic plot of the susceptibility spectrum for the correlator $\phi(t)$ (curve G of figure 4b in [9]). In these cases one knows that $\lambda = 0.7$ and the values for the non-ergodicity parameters f_c, f_c^s. Because of the universality of the β-process no further

Table 5. Coefficients required to evaluate the low-frequency result of the susceptibility, the von Schwindler behaviour and the latter's first correction term. See the text for details.

λ	B_0''	B_1''	B_0'	B_1'	ω^*	χ^*
0.500	0.228	2.193	0.000	−0.000	0.598	1.194
0.520	0.250	2.032	0.016	−0.126	0.637	1.198
0.540	0.273	1.888	0.034	−0.232	0.679	1.201
0.560	0.298	1.747	0.055	−0.320	0.725	1.204
0.580	0.324	1.618	0.079	−0.394	0.775	1.207
0.600	0.351	1.499	0.107	−0.456	0.831	1.209
0.620	0.381	1.386	0.139	−0.507	0.893	1.211
0.640	0.411	1.281	0.176	−0.550	0.966	1.213
0.660	0.445	1.182	0.220	−0.584	1.050	1.215
0.680	0.480	1.091	0.270	−0.613	1.151	1.217
0.700	0.517	1.007	0.327	−0.637	1.271	1.218
0.720	0.558	0.926	0.396	−0.656	1.420	1.219
0.740	0.602	0.851	0.475	−0.672	1.607	1.220
0.760	0.651	0.780	0.570	−0.684	1.850	1.221
0.780	0.704	0.713	0.684	−0.693	2.119	1.222
0.800	0.762	0.650	0.822	−0.701	2.624	1.223
0.820	0.828	0.590	0.992	−0.708	3.273	1.224
0.840	0.903	0.533	1.207	−0.712	4.282	1.224
0.860	0.990	0.479	1.483	−0.717	5.982	1.225
0.880	1.093	0.426	1.852	−0.722	9.178	1.225
0.900	1.218	0.374	2.366	−0.727	16.315	1.225
0.910	1.293	0.349	2.707	−0.731	23.517	1.225
0.920	1.378	0.324	3.129	−0.735	36.761	1.225
0.930	1.478	0.299	3.666	−0.741	64.049	1.225

Table 6. Moments for the low-frequency susceptibility (equation (19)). See the text for details.

λ	C_0	C_1	C_2	λ	C_0	C_1	C_2
0.500	0.805	0.48	0.49	0.740	0.312	0.10	0.05
0.520	0.767	0.44	0.43	0.760	0.269	0.08	0.03
0.540	0.729	0.41	0.40	0.780	0.228	0.06	0.02
0.560	0.690	0.38	0.35	0.800	0.187	0.04	0.01
0.580	0.651	0.35	0.32	0.820	0.149	0.03	0.01
0.600	0.610	0.32	0.28	0.840	0.113	0.02	0.01
0.620	0.569	0.28	0.24	0.860	0.080	0.01	0.00
0.640	0.527	0.25	0.20	0.880	0.051	0.00	0.00
0.660	0.484	0.21	0.15	0.900	0.028	0.00	0.00
0.680	0.441	0.18	0.12	0.910	0.019	0.00	0.00
0.700	0.398	0.15	0.09	0.920	0.012	0.00	0.00
0.720	0.355	0.12	0.07	0.930	0.007	0.00	0.00

details of the models are of interest here. The details merely enter the corrections to the asymptotic laws. The scales t_σ and hc_σ have to be fitted if one wants to connect the master curves g and χ'' of figures 1 and 3 via (1*a*) and (1*b*) to the quoted results. This is done by fitting two values for the result in figures 4 and 5 and by fitting the minimum in figure 6. In the latter case the fit merely amounts to a parallel shift of

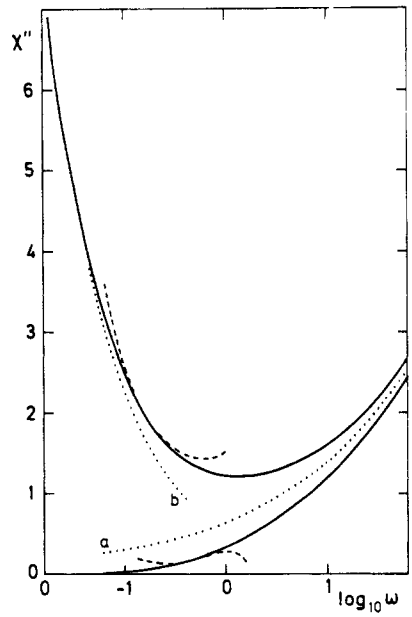

Figure 3. Master susceptibility spectrum χ'' versus $\log_{10}\omega$ for $\lambda = 0.7$. The broken curves are the various asymptotes discussed in the text. The dotted curve denoted by a is the critical spectrum $A_0''\omega^a$ and the one denoted by b is the von Schweidler spectrum B_0''/ω^b. The upper curves refer to the liquid $\epsilon = 1$, the lower ones to the glass $\epsilon = -1$.

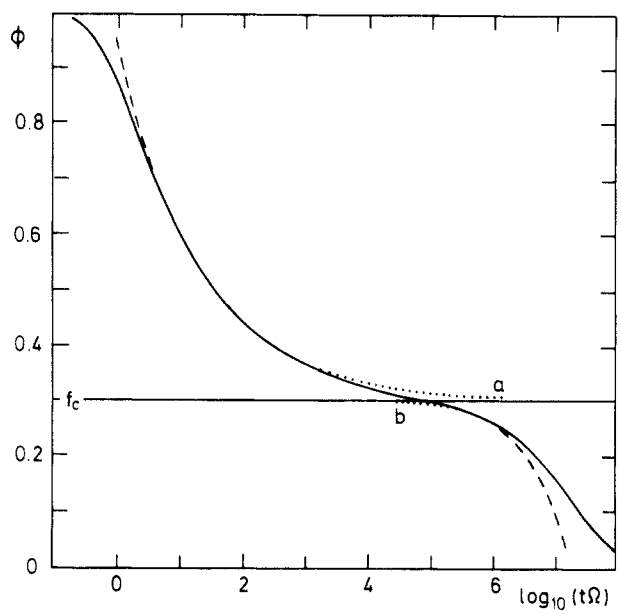

Figure 4. Density correlator ϕ as function of time from reference [9]. The broken curve exhibits the scaling law, $(1a)$ and $(1b)$, for $\lambda = 0.7$. The dotted curves represent the leading power-law asymptotes. See text.

the master curve without changing its shape. One recognizes that the curves ϕ, ϕ^s and χ'' follow the asymptotic results respectively over 5.5, 4.5 and 4 decades. The leading power-law asymptotes $1/t^a, A_0''\omega^a$ and $-Bt^b, B_0''/\omega^b$ are indicated by dotted lines. Notice that on the basis of these asymptotes, the only information which was available in the previous work, one cannot really judge the relevance of formulae (1). Notice in particular that in figure 4 one can identify the critical decay, specified by the anomalous dimensionality a, but not the von Schweidler law, characterized by the fractal dimensionality b. For figure 5 there holds the opposite. Since f_c is rather small in figure 4, corrections to the scaling-law influence the long-time behaviour strongly. In figure 5 the corresponding quantity f_c^s is big, and this is the reason for the von Schweidler law showing up so clearly.

The strong deviations from the critical decay law, shown in figure 5, are caused by the β-peak phenomenon [10]. The latter appears if one set of modes, represented

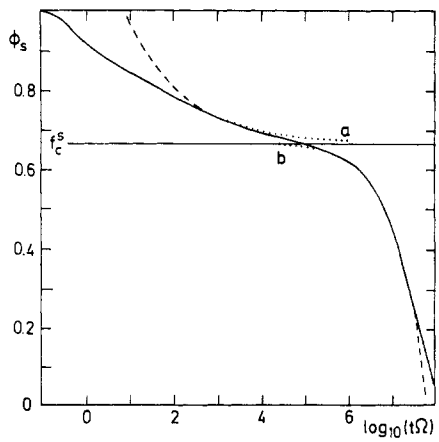

Figure 5. Tagged particle density correlator ϕ_s as function of time from reference [10]. The other symbols are used as in figure 4.

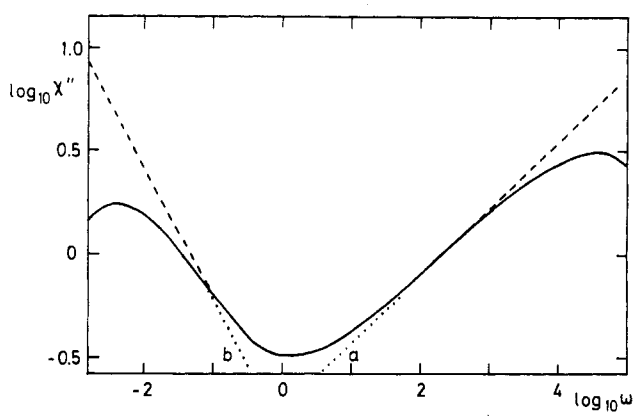

Figure 6. Susceptibility spectrum of the correlator from figure 4 taken from [9]. The broken lines are the scaling-law results for $\lambda = 0.7$. The dotted lines are the scaling-law asymptotes with slopes a and b, respectively.

here by ϕ^s, couples very strongly and asymmetrically to the density fluctuations, represented here by ϕ. In the limit of strong coupling one can work out the β-peak susceptibility with the result [11]:

$$\tilde{\chi}_\beta(\tilde{z}) = 1/[1 + (\nu/\Gamma(1-a))(-\tilde{z}\tau_\nu)g(\tilde{z}\tau_\nu)]\,. \tag{20a}$$

Here $\tilde{\chi}_\beta = \chi^s/C_1$ is the normalized dimensionless susceptibility of the distinguished variable; $\tilde{z} = z/C_2$ is the dimensionless frequency of the system. ν is a correlation scale related to the separation parameter ϵ by

$$\nu = C_3\sqrt{|\sigma|}. \tag{20b}$$

Quantity σ measures the distance from the underlying bifurcation singularity of the theory. If one considers the temperature T as control parameter one can choose $\sigma = (T_c - T)/T_c$, with T_c denoting the crossover temperature. The remainding parameter is the dimensionless scaling time t_σ of (1*b*), which can be expressed in terms of ν and the critical exponent a by

$$1/\tau_\nu = \nu^{1/a}. \tag{20c}$$

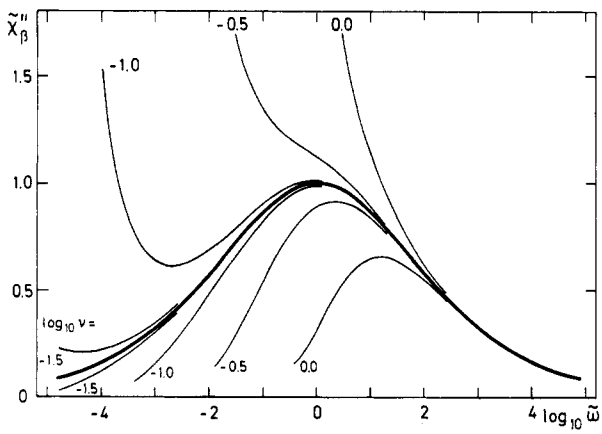

Figure 7. β-peak susceptibility spectra according to (20*a*) for $\lambda = 0.7$. The bold curve is the Cole–Cole result for $\nu = \sigma = 0$. The curves above and below the $\sigma = 0$ curve refer to liquid and glass for various separation parameters $|\sigma| \propto \nu^2$.

Asymptotically, C_1, C_2, and C_3 are just positive numbers representing the link between the physics of a many particle system and the simple mathematical expression (20*a*). In realistic application one is not working in the strict asymptotic limit $\sigma \to 0$. Then one can extend the range of applicability of the theory by incorporating e.g. temperature dependencies of the various parameter like C_1 to C_3. But these dependencies are smooth ones. All the sensitive variations, reflecting the bifurcation dynamics under study, are contained explicitly in the formula (20). C_1 links e.g. the systems dipole moment with the correlator of the theory. C_2 connects the microscopic internal time scale with the model parameter t. C_3 connects the temperature with the mathematical control parameter ν. It is a non-trivial prediction of the mode coupling theory that no other information enters the result, except for the all important exponent

parameter λ. The latter determines exponent a in (20a) and (20c) and it fixes the master function $\tilde{\omega}g(\tilde{\omega})$. The results of this paper yield $g(\tilde{\omega})$ and figure 7 shows the β-peak scenario for $\lambda = 0.7$. In the limit $\nu \to 0$ the β-peak is described by the Cole–Cole law $\tilde{\chi} = 1/[1 + (-i\tilde{z})^a]$ [11]. This function is shown as the heavy line in the figure; it is a symmetric peak on a logarithmic frequency axis whose half width is as large as 4.6 decades. If $-\sigma$ increases the susceptibility spectrum becomes larger, the resonance broadens and then it is changed to a shoulder. This phenomenon is observed regularly and it simply means that the β-peak disappears under the von Schweidler tail of the α-resonances. The theory under discussion predicts the quantitative details of this phenomenon. It predicts in particular that in those cases where there is no β-peak at all, there should be a crossover from a $1/\omega^b$ fractal spectrum to a $1/\omega^a$ fractal. The former is the high-frequency tail of the α-peak and the latter is the high-frequency wing of the β-peak. The fractal exponents are related by (7). A corresponding spectrum is shown for $\nu = 1$ in figure 7. The conventional semi logarithmic presentation does not exhibit the $1/\omega^b$ to $1/\omega^a$ crossover so clearly. As usual, a power-law crossover can only be clearly seen on a double logarithmic plot. On the low-temperature side of the transition two important effects are exhibited in the figure. The left wing of the resonance gets suppressed. With increasing σ the β-peak becomes more and more asymmetric and gets a form which is familiar from the α-resonances. Furthermore the peak height gets lowered. These effects are shown by the dielectric loss data for polyvinyl acetate, to mention just one experimental result [12]. The mode-coupling theory explains qualitatively how one arrives from Newton's equations of motion via some universal scaling equation to resonance peaks with the well known glass dynamics signature. In particular, it identifies fractal time dynamics as resulting from the interplay of non-linear coupling with retardation phenomena. The fractals found result, even though there is no fractal structure in the underlying configuration space. The fractals are the true reason for the stretching of the relaxation over many decades, as shown in the figures and detected for the β-peak in [12].

References

[1] Götze W 1987 *Amorphous and Liquid Materials* ed E Lüscher, G Fritsch and G Jacucci (Dordrecht: Martinus Nijhoff) p 34

[2] Sjögren L and Götze W 1989 *Dynamics of Disordered Materials* ed D Richter, A J Dianoux, W Petry and J Teixeira (Berlin: Springer) p 18

[3] Knaak W, Mezei F and Farago B 1988 *Europhys. Lett.* **7** 529

[4] Sjögren L 1990 *Basic Features of the Glassy State* ed J Colmenero and A Alegria (Singapore: World Scientific) p 137

[5] Knaak W 1989 *Dynamics of Disordered Materials* ed D Richter, A J Dianoux, W Petry and J Teixeira (Berlin: Springer) p 164

[6] Roux J N, Barrat J L and Hansen J P 1989 *J. Phys.: Condens. Matter* **1** 7171

[7] Pusey P N and van Megen W 1990 *Ber. Bunsenges. Phys. Chem.* **94** 225

[8] Götze W 1984 *Z. Phys.* B **56** 139

[9] Götze W and Sjögren L 1988 *J. Phys. C: Solid State Phys.* **21** 3407

[10] Buchalla G, Dersch U, Götze W and Sjögren L 1988 *J. Phys. C: Solid State Phys.* **21** 4239

[11] Götze W and Sjögren L 1989, *J. Phys.: Condens. Matter* **1** 4183

[12] Ishida Y, Matsuo M and Yamafuji K 1962 *Kolloid Z.* **180** 108